Instantons, Fluctuations, and Singularities in the Supercritical Stochastic Nonlinear Schrödinger Equation

Sumeja Bureković,[1,*] Tobias Schäfer,[2,3,†] and Rainer Grauer[1,‡]
[1]Institute for Theoretical Physics I, Ruhr University Bochum, Universitätsstrasse 150, D-44801 Bochum, Germany
[2]Department of Mathematics, College of Staten Island, Staten Island, New York 10314, USA
[3]Physics Program, CUNY Graduate Center, New York, New York 10016, USA

(Received 2 February 2024; accepted 10 July 2024; published 15 August 2024)

Recently, Josserand *et al.* proposed a stochastic nonlinear Schrödinger model for finite-time singularity-mediated turbulence [Phys. Rev. Fluids **5**, 054607 (2020)]. Here, we use instanton calculus to quantify the effect of extreme fluctuations on the statistics of the energy dissipation rate. While the contribution of the instanton alone is insufficient, we obtain excellent agreement with direct simulations when including Gaussian fluctuations and the corresponding zero mode. Fluctuations are crucial to obtain the correct scaling when quasisingular events govern the turbulence statistics.

DOI: 10.1103/PhysRevLett.133.077202

Introduction—Understanding non-Gaussian statistics and anomalous scaling in turbulent systems is one of the outstanding challenges in classical physics [1]. Given that the underlying probability distributions in such turbulent systems are dominated by extreme fluctuations, different toy models have been proposed, among them the stochastic Burgers [2], the Kuramoto-Sivashinsky [3], and, more recently, the nonlinear Schrödinger equation (NLS) [4–6]. In this Letter, our work focuses on the NLS, although the presented methods can be applied to a wide range of turbulent models. Recall that the NLS naturally arises in a variety of contexts, in particular in nonlinear optics [7–9] and plasma physics [10,11], and has come into the focus of novel applications in the context of Bose-Einstein condensates [12], optical turbulence [13], and rogue waves [14].

The one-dimensional stochastic focusing NLS on a spatial domain of size ℓ, as introduced in [6], is given by

$$\partial_t\psi = \frac{\mathbb{i}}{2}\partial_x^2\psi + \mathbb{i}|\psi|^6\psi - \nu\partial_x^4\psi + \chi^{1/2} * \eta, \tag{1}$$

$$\psi(\cdot, t=0) = 0, \tag{2}$$

where $*$ denotes spatial convolution and $\chi^{1/2} * \chi^{1/2} = \chi$. The first three terms of Eq. (1) describe the self-focusing conservative NLS with a supercritical nonlinearity [15]. The remaining two terms constitute hyperviscous damping with hyperviscosity ν and a complex Gaussian forcing $\mathbb{E}[\eta(x,t)\eta^*(x',t')] = 2\sigma^2\delta(x-x')\delta(t-t')$ that is white in time and has large-scale spatial correlations χ with amplitude σ.

In [6] it was proposed that the nearly singular collapsing solutions of the NLS (1) provide a skeleton for the emergence of intermittency in the strongly turbulent case. In the present Letter, we will analyze the turbulence statistics of the NLS (1) via instanton calculus to support the notion of singularity mediated turbulence as introduced in [6].

The general picture of [6] is consistent with the reasoning in hydrodynamic and magnetohydrodynamic turbulence, where the nearly singular structures such as shocks, vortices, or current sheets play a similar role. The important role of structures in understanding turbulent systems has already been suggested in the justification of the multifractal picture of turbulence [16] and later incorporated in phenomenological models of turbulence [17,18] and in the understanding of anomalous dissipation [19]. Another indication of the importance of the nearly singular structures is found in [20], where a combination of local and nonlocal nonlinearity allows the regularity of the singularity to change, leading to intermittency of varying strength.

The NLS turbulence differs from the usual Navier-Stokes turbulence in two major ways. First, the NLS has two (instead of one, as in Navier-Stokes turbulence) independent dimensionless parameters: In Eq. (1), one can specify the system size and choose the viscosity ν and forcing strength σ as independent parameters. Another possibility would be to fix ν and vary the system size and σ. This has also been discussed for the two-dimensional focusing NLS [21].

The second, more important difference to the Navier-Stokes equations is the existence of a blow-up criterion for the critical mass in the focusing NLS, which determines

*Contact author: sumeja.burekovic@ruhr-uni-bochum.de
†Contact author: tobias.schaefer@csi.cuny.edu
‡Contact author: grauer@tp1.rub.de

whether initial configurations remain regular or form singularities in finite time (cf. [15]). This particular property of the NLS has a significant impact on turbulence characteristics such as the probability distribution of local energy dissipation, as will become evident when discussing the main result.

Since instantons are the most probable space and time dependent field configurations for given strong events associated with singular structures, their use in explaining this type of singularity mediated turbulence seems a natural choice. In contrast to fluid turbulence, where many other complex dynamical processes can occur in addition to the development of vortex tubes or sheets, e.g., topology-changing reconnection events, the tendency for singularity formation in the NLS is so robust that it dominates the turbulent dynamics. Our analysis supports this viewpoint and shows that NLS turbulence is accessible through the instanton approach, when including Gaussian fluctuations and zero modes.

In this Letter, we quantify the effect of extreme fluctuations on NLS turbulence by considering the tails of the probability density function (PDF) of the energy dissipation density ε [6], defined as

$$\varepsilon(x,t) = 2\nu|\partial_x^2\psi(x,t)|^2. \tag{3}$$

We analyze the PDF ρ of ε, as further statistical quantities can be derived from it. To compute ρ, we apply the instanton approach (cf. [22] and references therein), which consists of the following steps: (i) find the instanton as the minimizer of the action in the corresponding path integral, (ii) compute the Gaussian fluctuations around the instanton that lead to a fluctuation determinant, (iii) add contributions from possible zero modes. This approach corresponds to large deviation theory in mathematics [23,24]. While the road map (i)–(iii) has been known—in principle—for decades, this program could not be successfully applied in the context of turbulent systems due to the lack of appropriate numerical methods and computational power. Nowadays, however, both are available. Nevertheless, it should be noted that in the case of the direct cascade in two-dimensional Navier-Stokes turbulence fluctuations have already been used to determine an effective action and account for the universal exponential shape of the vorticity PDF [25].

All of these steps (i)–(iii) can be carried out in different ways, and each method has its advantages for a particular application. The path integral for stochastic differential equations can, e.g., be formulated as the Onsager-Machlup path integral [26,27] or the Janssen–de Dominicis path integral [28,29] by applying a Hubbard-Stratonovich transformation. In the following, limiting expressions for the PDF are derived analytically and evaluated numerically. Here, we use the path integral over all noise realizations, since the noise considered here mimics a large-scale forcing and hence, this formulation has computational advantages over the more general approaches [30–32] when calculating the fluctuation determinant (see Ref. [33] for details). Thus, the PDF of the energy dissipation density ε at a value a reads

$$\rho(a) = \int \mathcal{D}\eta \exp\left(-\frac{1}{2\sigma^2}\|\eta\|_{L^2}^2\right)\delta(F[\eta]-a), \tag{4}$$

with $\langle\cdot,\cdot\rangle_{L^2}$ denoting the L^2 product in space and time. The central object in this path integral is the solution map F that solves the NLS (1) for a given input noise η, and returns the observable value: $F[\eta] = O[\psi[\eta](\cdot,T)]$ at a final time $T > 0$. Here, we take the energy dissipation density as $O[\psi(\cdot,T)] = \varepsilon(0,T)$, where the choice $x = 0$ is without loss of generality due to the homogeneity of the problem, and T was chosen sufficiently large compared to the typical collapse time.

In the constraint $O[\psi(\cdot,T)] = a$, the interest is in extreme events, i.e., in large values of a as it was introduced for Burgers turbulence [34–37] almost 30 years ago. Formally, we take the small noise limit $\sigma\downarrow 0$, which is equivalent as long as a is sufficiently large (cf. [30]). By Laplace's method, the path integral (4) will have the following asymptotic form:

$$\rho(a) = C(a)\exp\left(-\frac{S_{\mathrm{I}}(a)}{\sigma^2}\right)(1+\mathcal{O}(\sigma^2)), \tag{5}$$

as $\sigma\downarrow 0$, where we call $C(a)$ the algebraic prefactor, and the exponential contribution stems from the instanton. While there are results on instantons in the NLS [14,38–43] neither the specific supercritical form (1), nor the energy dissipation density observable, have been considered so far. More importantly, to the best of our knowledge, the computation of the PDF prefactor C for the NLS (1) is a novelty as well and turns out to be crucial. In the following, we briefly explain how we obtain both the instanton and the prefactor contributions.

(i) Instanton—In the path integral (4), the instanton is the minimizer of the action functional with observable constraint:

$$S_{\mathrm{I}}(a) = \min_{\eta\,\mathrm{s.t.}\,F[\eta]=a} S[\eta], \qquad S[\eta] = \frac{1}{2}\|\eta\|_{L^2}^2. \tag{6}$$

For increased numerical efficiency and stability, in order to find the optimal η, we do not directly solve the corresponding Euler-Lagrange or instanton equations, but use optimal control methods with control variable η, similarly to [44]. By this we iteratively solve a deterministic forward and backward PDE of very similar shape and perform unconstrained optimization as follows:

First, we write the constraint in Eq. (6) as a Lagrange term in the functional $R_\lambda[\eta] = S[\eta] - \lambda(F[\eta]-a)$ with a Lagrange multiplier λ. Since the instanton action S_{I} will

turn out to be non-convex in a (cf. [43]), we use an augmented Lagrangian [45] with a penalty parameter μ:

$$R[\eta] = S[\eta] - \lambda(F[\eta] - a) + \frac{\mu}{2}(F[\eta] - a)^2. \tag{7}$$

For sufficiently large μ, the instanton solution of equation (6) for an observable value a, is $\eta_a = \mathrm{argmin}_\eta R[\eta]$. We perform a gradient-based minimization of R, thus we need $\delta F/\delta\eta$. To evaluate this complicated expression, we employ the adjoint-state method [46] by using a field-valued Lagrange multiplier z. Details are given in the Supplemental Material [47]. In total, the gradient reads

$$\frac{\delta R}{\delta \eta} = \eta - \chi^{1/2} * z, \tag{8}$$

where z solves

$$\partial_t z - \frac{\mathrm{i}}{2}\partial_x^2 z - \nu\partial_x^4 z - 4\mathrm{i}|\psi|^6 z + 3\mathrm{i}|\psi|^4\psi^2 z^* = 0, \tag{9}$$

$$z(x,T) = 4\nu(\lambda - \mu(\varepsilon(0,T) - a))\partial_x^2\psi(0,T)\delta''(x), \tag{10}$$

with $\psi = \psi[\eta]$ through Eq. (1). At the instanton, by the first-order optimality condition, the gradient (8) is zero, i.e., $\eta_a = \chi^{1/2} * z_a$. Substituting this expression for z in the adjoint PDE (9) yields the instanton or Hamilton equations with the optimal η_a corresponding to the optimal conjugated momentum of the system up to a factor $\chi^{1/2}$.

For a fixed observable value a, the instanton η_a, from which $S_\mathrm{I}(a)$ is obtained, is found by solving a series of unconstrained optimization problems $\min_\eta R[\eta]$ for increasing values $\mu^{(i)}$ of the penalty parameter, and the Lagrange multiplier is updated according to [[45], p. 515]. For each evaluation of the gradient (8), we first solve the forward equation (1) and then the adjoint equation (9).

We implemented a pseudospectral code to solve these equations with a 1/4 anti-aliasing [51]. In line with [44], we use the L-BFGS scheme [52] for the minimization in real variables. For this, we write all complex fields as two-dimensional real vectors, as shown in the Supplemental Material [47]. The optimization code has been consistently discretized, with the Heun scheme with integrating factor for the forward equation.

(ii),(iii) Gaussian fluctuations and zero mode—Now, we compute an estimate of the prefactor C in Eq. (5). All formulas are given for $a > 0$. For this computation, we employ the approach based on Fredholm determinants established in [33]. After calculating the instanton solutions ψ_a^φ, η_a^φ, and z_a^φ, we insert these fields as background fields in the computation of the prefactor. Since the NLS (1) as well as the observable function (3) are globally U(1) invariant with respect to the complex phase $\varphi = \arg(\psi)$, the instanton solution is degenerate in φ and therefore gives rise to a zero mode which we indicate by the superscript φ. Because of the zero mode, the Fredholm determinant in [33] is ill defined and has to be regularized. For this, we follow [53].

We split the domain of integration of the path integral (4) into the submanifold M^1 of the instanton (noise) solutions η_a^φ, and the subspace $N_\varphi M^1$ that is normal (with respect to the L^2 product) to the zero mode: $\eta \to \eta_a^\varphi + \sigma\tilde{\eta}$. The submanifold $M^1 = \mathrm{argmin}_\eta S[\eta]$ is one dimensional since the zero mode stems from the scalar parameter φ. The split of integration directions is usually done formally using the Faddeev-Popov method [54]. As detailed in the Supplemental Material [47], the leading-order prefactor C in formula (5) then reads

$$C(a) = \frac{1}{\sigma^2}|\lambda_a|\det{}'(\mathrm{Id} - B_a)^{-1/2}. \tag{11}$$

The Lagrange multiplier $\lambda_a = \mathrm{d}S_\mathrm{I}/\mathrm{d}a$ is obtained from the optimization scheme given above. The regularized Fredholm determinant $\det'$ is approximated using the largest eigenvalues $\kappa_a^{(i)} \neq 1$ of the operator B_a, given by

$$B_a = \lambda_a \mathrm{pr}_{\eta_a^\perp} \frac{\delta^2 F}{\delta\eta^2}\bigg|_{\eta=\eta_a} \mathrm{pr}_{\eta_a^\perp}, \tag{12}$$

with the projection operator $\mathrm{pr}_{\eta_a^\perp}$ defined in the Supplemental Material [47]. These eigenvalues are calculated iteratively [50] from the solution of second-order equations [33], which are given in the Supplemental Material [47]. In Fig. 1, we show the convergence of the numerical approximation of $\det'(\mathrm{Id} - B_a)$ for an example observable value.

Direct numerical simulations (DNS)—We also performed Monte Carlo simulations of the NLS (1) with

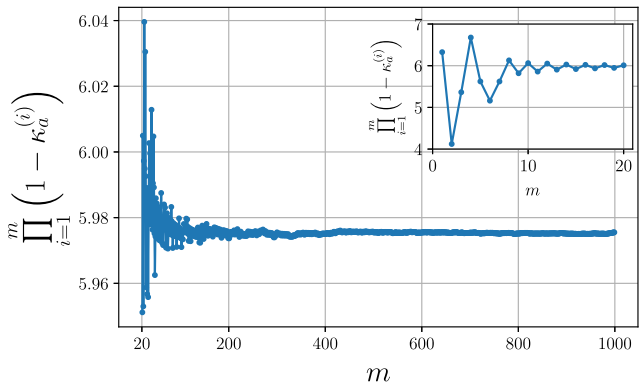

FIG. 1. Result of numerically computing the $m = 1000$ eigenvalues $\kappa_a^{(i)}$ of B_a with the largest absolute value for $\varepsilon(0,T) = a = 0.015$. The figure shows the finite product $\prod_{i=1}^{m}\left(1-\kappa_a^{(i)}\right)$ approximating the regularized Fredholm determinant $\det'(\mathrm{Id} - B_a)$ without the zero mode $\kappa_a = 1$. The numerical approximation of $\det'(\mathrm{Id} - B_a)$ converges quickly. All subsequent results in this Letter are obtained for $m = 1000$.

TABLE I. Parameters that enter the DNS, the optimization scheme for the instanton computation, and the computation of the Gaussian fluctuations.

Parameter	Definition	Value
ℓ	Length of periodic spatial domain	153.6
ν	Hyperviscosity	10^{-2}
T	Time interval $[0, T]$	2.0
N_t	Time resolution	2^{12}
N_x	Spatial resolution	2^{12}

the same parameters as for the instanton and fluctuation computations, which are given in Table I. Following [6], we only force large length scales: $\hat{\chi}_k = (1/\ell)\mathbb{1}_{[0<|k|<0.3(\ell/2\pi)]}$ for $k \in \mathbb{Z}$. To compute the PDF ρ from DNS data, we used 9.3×10^6 simulated fields and evaluated 3.7×10^8 statistically independent samples.

Discussion of results—The main result is shown in Fig. 2, which displays the PDF for the energy dissipation density (3). In this figure, the noise strength is given by $\sigma^2 = 0.5$. Other values of the noise strength ($\sigma^2 = 0.4$, $\sigma^2 = 0.75$) were studied as well and show a very similar behavior. Two regions can be identified: A region belonging to smaller values of energy dissipation ($a \leq 2 \times 10^{-5}$) and a region of rare fluctuations of the energy dissipation ($4 \times 10^{-5} \leq a \leq 10^{-2}$). In the first region, the PDF calculated from the DNS agrees almost exactly with the asymptotic prediction of the instanton calculation including the fluctuations. However, even the prediction of the PDF using solely the instanton with a constant prefactor C in Eq. (5), instead of the full expression (11), yields a result

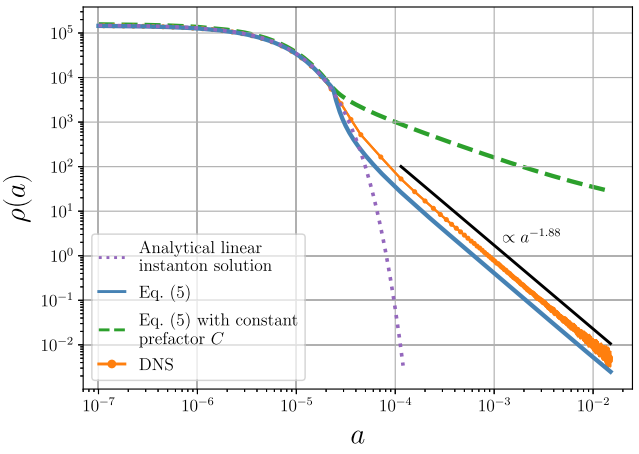

FIG. 2. Comparison of instanton predictions and DNS results for the PDF ρ of the energy dissipation density (3). The dashed line indicates the leading order contribution $\exp(-S_I/\sigma^2)$ in Eq. (5) with a constant prefactor instead of Eq. (11). The shaded regions for the DNS data are 99% Wilson score intervals [55]. The DNS data and full instanton prediction show a power-law decay for large a with scaling exponent ≈1.88.

indistinguishable from the DNS. A typical instanton evolution is shown in the left part of Fig. 3.

To understand this observation, we analytically solved the instanton equations and computed the prefactor in case of vanishing nonlinearity, which is given in the Supplemental Material [47]. The resulting prediction for the PDF, an exponential distribution, is also shown in Fig. 2 and again agrees well with the DNS result in the first region. This can be explained by the fact that in the first region, the corresponding instanton is below the critical mass that would lead to a collapse, such that the focusing nonlinearity effectively vanishes. We tested this hypothesis numerically by setting the instantons in this parameter range as initial conditions in the deterministic conservative NLS ($\sigma = \nu = 0$). Indeed, the numerical solution produced no collapse in this region. This range therefore corresponds to an almost linear regime in which the instanton prediction is nearly exact, i.e., the small noise limit is almost perfectly fulfilled.

The result in the second region is even more surprising. In this region, there is initially no agreement between the results of the DNS and the prediction of the PDF by the instanton without the fluctuations. Note that this curve can be shifted arbitrarily on the vertical axis, since the normalization of the PDF is not determined by the instanton itself. In this range ($4 \times 10^{-5} \leq a \leq 10^{-2}$), the PDF of the energy dissipation shows a power law behavior (cf. [4,5]), i.e., it is completely dominated by the prefactor and the exponential part due to the instanton alone is subdominant. The agreement of the power law scaling prediction of the instanton calculation including the fluctuations and the DNS is almost perfect (with convergence of the two curves—instanton prediction and extrapolated DNS data—for even larger a). Our interpretation of this result is given by the special characteristic of the focusing NLS to form strongly localized structures. Also, in this parameter range, we used the instantons as initial conditions in the conservative and deterministic NLS. Here, unlike the first region, these initial conditions led to a collapse. A typical instanton in this regime is depicted in the right of Fig. 3. In contrast to other turbulent systems, the NLS turbulence is characterized by the occurrence of localized, spatially

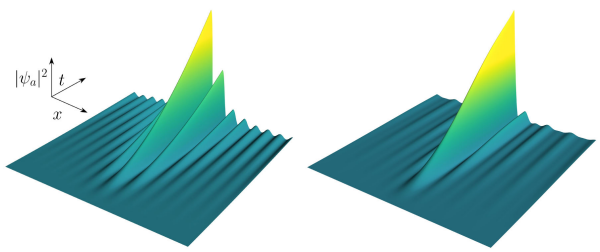

FIG. 3. Spatiotemporal surface plots of instanton fields ψ_a for $a = 2 \times 10^{-5}$ (left) and $a = 0.015$ (right). As a scale reference, $\max_{x,t}|\psi_a|^2 \approx 0.34$ (left) and $\max_{x,t}|\psi_a|^2 \approx 1.55$ (right).

barely interacting nearly singular structures. This is particularly well illustrated in Fig. 1 of the work of Josserand *et al.* [6]. We can also interpret this property of the collapsing NLS as the fact that the action landscape in the path integral formulation exhibits strongly localized extrema, which can be very well represented by a Gaussian approximation around the instanton.

Conclusions and outlook—In this Letter we illuminated a promising pathway to understand intermittency in turbulent system from first principles. In the case of the stochastic supercritical NLS considered here, the instanton formalism is able to capture precisely the PDF of the energy dissipation (3), which is far from a Gaussian distribution, and gives the correct scaling in the strongly nonlinear region. The decisive factor was the inclusion of the Gaussian fluctuations around the instanton and the consideration of the zero mode in our analysis. In contrast to phenomenological approaches incorporating singular structures, we obtain all information of the system like probability densities directly from the underlying equations of motion. In some way, this case can be considered as a paradigm for turbulence that is dominated by isolated weakly singular structures. This differs from the situation in real turbulence as it occurs, for example, in the Navier-Stokes equations. But even in the simpler case of shock-dominated Burgers turbulence, the situation is more complex, so that there are significant deviations in the gradient statistics at higher Reynolds numbers between the predictions of the instanton formalism and the results of numerical simulations. For instance, shocks can merge in the Burgers turbulence and thus have a further influence on the gradient statistics. The situation is even more complex in Navier–Stokes turbulence, where reconnection of vortex tubes and other, more complex processes can occur. Such events are not yet included in the instanton formalism. The transition between Gaussian PDFs in the realm of small observable values and the PDFs associated with large observable values dominated by singularities remains a challenge. Our approach paves the way to move in this direction. One possibility would be to weaken the nonlinearity in the NLS towards the critical case. This would reduce the nature of the extreme singularities and could therefore systematically lead towards more complex interactions. Research in this direction is in progress.

Acknowledgments—The authors would like to thank Timo Schorlepp for helpful discussions on the Fredholm determinant prefactor. R. G. acknowledges support from the German Research Foundation DFG within the Collaborative Research Center SFB1491. T. S. acknowledges support from the NSF Grant No. DMS-2012548.

[1] U. Frisch, *Turbulence: The Legacy of A. N. Kolmogorov* (Cambridge University Press, Cambridge, England, 1995).
[2] J. M. Burgers, Adv. Appl. Mech. **1**, 171 (1948).
[3] P. Manneville, Phys. Lett. **84A**, 129 (1981).
[4] Y. Chung, P. M. Lushnikov, and N. Vladimirova, AIP Conf. Proc. **1168**, 1235 (2009).
[5] Y. Chung and P. M. Lushnikov, Phys. Rev. E **84**, 036602 (2011).
[6] C. Josserand, Y. Pomeau, and S. Rica, Phys. Rev. Fluids **5**, 054607 (2020).
[7] V. E. Zakharov and A. B. Shabat, Sov. Phys. JETP **34**, 62 (1972), https://zakharov75.itp.ac.ru/static/local/zve75/zakharov/1972/1972-05-e_034_01_0062.pdf.
[8] A. Hasegawa and Y. Kodama, *Solitions in Optical Communications* (Clarendon Press, Oxford, 1995).
[9] G. P. Agrawal, *Nonlinear Fiber Optics*, 6th ed. (Academic Press, New York, 2019).
[10] V. E. Zakharov, Sov. Phys. JETP **35**, 908 (1972), https://zakharov75.itp.ac.ru/static/local/zve75/zakharov/1972/1972-04-e_035_05_0908.pdf.
[11] S. Novikov, S. Manakov, L. Pitaevskii, and V. Zakharov, *Theory of Solitons: The Inverse Scattering Method*, Monographs in Contemporary Mathematics (Springer, New York, 1984).
[12] F. Dalfovo, S. Giorgini, L. P. Pitaevskii, and S. Stringari, Rev. Mod. Phys. **71**, 463 (1999).
[13] S. Dyachenko, A. Newell, A. Pushkarev, and V. Zakharov, Physica (Amsterdam) **57D**, 96 (1992).
[14] G. Dematteis, T. Grafke, M. Onorato, and E. Vanden-Eijnden, Phys. Rev. X **9**, 041057 (2019).
[15] G. Fibich, *The Nonlinear Schrödinger Equation: Singular Solutions and Optical Collapse* (Springer, New York, 2015).
[16] U. Frisch and G. Parisi, in *Proceedings of the Turbulence and Predictability in Geophysical Fluid Dynamics and Climate Dynamics* (Elsevier, Amsterdam, The Netherlands, 1985), pp. 84–88.
[17] Z.-S. She and E. Leveque, Phys. Rev. Lett. **72**, 336 (1994).
[18] R. Grauer, J. Krug, and C. Marliani, Phys. Lett. A **195**, 335 (1994).
[19] J. Duchon and R. Robert, Nonlinearity **13**, 249 (2000).
[20] O. Zikanov, A. Thess, and R. Grauer, Phys. Fluids **9**, 1362 (1997).
[21] J. Amauger, C. Josserand, Y. Pomeau, and S. Rica, Physica (Amsterdam) **443D**, 133532 (2023).
[22] T. Grafke, R. Grauer, and T. Schäfer, J. Phys. A **48**, 333001 (2015).
[23] S. R. S. Varadhan, *Large Deviations and Applications* (Society for Industrial and Applied Mathematics, Philadelphia, 1984).
[24] M. I. Freidlin and A. D. Wentzell, *Random Perturbations of Dynamical Systems*, 3rd ed., Grundlehren der mathematischen Wissenschaften (Springer, New York, 2012), Vol. 260.
[25] G. Falkovich and V. Lebedev, Phys. Rev. E **83**, 045301(R) (2011).
[26] L. Onsager and S. Machlup, Phys. Rev. **91**, 1505 (1953).
[27] S. Machlup and L. Onsager, Phys. Rev. **91**, 1512 (1953).
[28] H.-K. Janssen, Z. Phys. B Condens. Matter Quanta **23**, 377 (1976).
[29] C. de Dominicis, J. Phys. (Paris), Colloq. **37**, C1 (1976).

[30] T. Schorlepp, T. Grafke, and R. Grauer, J. Phys. A **54**, 235003 (2021).
[31] T. Grafke, T. Schäfer, and E. Vanden-Eijnden, Commun. Pure Appl. Math. **77**, 1 (2023).
[32] F. Bouchet and J. Reygner, J. Stat. Phys. **189**, 21 (2022).
[33] T. Schorlepp, S. Tong, T. Grafke, and G. Stadler, Stat. Comput. **33**, 137 (2023).
[34] V. Gurarie and A. Migdal, Phys. Rev. E **54**, 4908 (1996).
[35] G. Falkovich, I. Kolokolov, V. Lebedev, and A. Migdal, Phys. Rev. E **54**, 4896 (1996).
[36] E. Balkovsky, G. Falkovich, I. Kolokolov, and V. Lebedev, Phys. Rev. Lett. **78**, 1452 (1997).
[37] A. I. Chernykh and M. G. Stepanov, Phys. Rev. E **64**, 026306 (2001).
[38] G. E. Falkovich, I. Kolokolov, V. Lebedev, and S. K. Turitsyn, Phys. Rev. E **63**, 025601(R) (2001).
[39] I. S. Terekhov, S. S. Vergeles, and S. K. Turitsyn, Phys. Rev. Lett. **113**, 230602 (2014).
[40] M. Onorato, D. Proment, G. El, S. Randoux, and P. Suret, Phys. Lett. A **380**, 3173 (2016).
[41] G. Poppe and T. Schäfer, J. Phys. A **51**, 335102 (2018).
[42] G. Roberti, G. El, S. Randoux, and P. Suret, Phys. Rev. E **100**, 032212 (2019).
[43] M. Alqahtani and T. Grafke, J. Phys. A **54**, 175001 (2021).
[44] T. Schorlepp, T. Grafke, S. May, and R. Grauer, Phil. Trans. R. Soc. A **380**, 20210051 (2022).
[45] J. Nocedal and S. J. Wright, *Numerical Optimization*, 2nd ed. (Springer, New York, NY, USA, 2006).
[46] R.-E. Plessix, Geophys. J. Int. **167**, 495 (2006).
[47] See Supplemental Material at http://link.aps.org/supplemental/10.1103/PhysRevLett.133.077202, which includes Refs. [48–50], for additional information on the derivations and numerical methods.
[48] A. Lang and J. Potthoff, Monte Carlo Methods Appl. **17**, 195 (2011).
[49] T. Schorlepp, T. Grafke, S. May, and R. Grauer, Phil. Trans. R. Soc. A, 10.6084/m9.figshare.19329079.v1 (2022).
[50] R. B. Lehoucq, D. C. Sorensen, and C. Yang, *ARPACK Users' Guide* (Society for Industrial and Applied Mathematics, Philadelphia, 1998).
[51] D. Fructus, D. Clamond, J. Grue, and Ø. Kristiansen, J. Comput. Phys. **205**, 665 (2005).
[52] D. C. Liu and J. Nocedal, Math. Program. **45**, 503 (1989).
[53] T. Schorlepp, T. Grafke, and R. Grauer, J. Stat. Phys. **190**, 50 (2023).
[54] L. D. Faddeev and V. N. Popov, Phys. Lett. **25B**, 29 (1967).
[55] L. D. Brown, T. T. Cai, and A. DasGupta, Stat. Sci. **16**, 101 (2001).